Contributed paper

OPTO-ELECTRONICS REVIEW 7(4), 361–367 (1999)

Studies of relationship between deep levels and R_0A product in mesa type HgCdTe devices

J. YOSHINO[1*], J. MORIMOTO[1], H. WADA[2], A. AJISAWA[3], M. KAWANO[3], and N. ODA[3]

[1]Department of Materials Science and Engineering, National Defence Academy
1-10-20 Hashirimizu, Yokosuka, Kanagawa 239-8686, Japan
[2]Technical Research and Development Institute, Japan Defence Agency
1-2-24 Ikejiri, Setagaya, Tokyo 154-8511, Japan
[3]Material Development Centre, NEC Corporation
4-1-1 Miyazaki, Miyamae, Kawasaki, Kanagawa 216-8555, Japan

The relationships between the figure of merit R_0A representing the junction property and deep levels representing electric properties of semiconductors have been studied. R_0A can be estimated by current-voltage (I–V) measurements. Deep levels can be estimated using spectral analysis of deep level transient spectroscopy (SADLTS). It has been confirmed that values of activation energies concentrate around 30 meV with the increase of R_0A. This suggests that the influence from the inherent deep levels in the HgCdTe device becomes strong due to the increase of R_0A, resulting in the improvement of the diode characteristics.

Keywords: HgCdTe, DLTS, SADLTS, mesa-type, R_0A product, deep level, activation energy.

1. Introduction

The realised photoconductive devices using HgCdTe have usually the hybrid-type structure. However, the hybrid structure has the problem that devices are subjected to the mechanical damage due to the differences in the thermal expansion coefficients amongst HgCdTe, buffer layer and substrate when the devices are cooled down to the operating temperature, 77 K. Furthermore, CdZnTe widely used as the substrate is fragile compared with Si. It is also the problem that large focal plain arrays (FPAs) require high cost for materials preparation. Another problem is to control the conduction type for the planar-type HgCdTe devices by defects due to ion implantation. Then the damage induced by ion implantation may increase the dark current in the HgCdTe devices. In order to fabricate the high sensitivity photovoltaic devices, it is necessary to suppress the dark current.

The mesa-type HgCdTe devices, which have the monolithic structure, are studied to overcome the problems mentioned above [1]. Using the mesa-type structure, the epitaxial HgCdTe layer can be grown on the Si substrate, which is low cost material and widely used for a read-out circuit. However, the damage due to the surface current and etching may occur in the mesa-type HgCdTe devices.

The dark current contains the diffusion current, generation-recombination current and tunnelling current [2]. The dominance of the dark current has been investigated using fitting method [3]. The figure of merit of junction, R_0A, is related to the dark current. Therefore, when R_0A increases, the dark current should be decreased.

There are defects in the HgCdTe devices such as vacancies and dislocations, potential turbulence at the interface between HgCdTe and the Si substrate, and the mechanical and chemical damage during the mesa fabrication. Then these may be the origins of deep levels in the HgCdTe devices. Estimating deep levels is important to evaluate characteristics of semiconductors since deep levels are related to electric properties of devices.

*e-mail: jyoshino@cc.nda.ac.jp

Deep levels in semiconductors are described by Shockley-Read-Hall (SRH) statistics. It is considered that the trap-assisted tunnelling current is concerned to these levels acting as the trap centres [4]. Thus it is expected that there is some relationship between R_0A and deep levels that are related to the dark current.

In this work, the relationships between R_0A and deep levels have been studied using spectral analysis of deep level transient spectroscopy (SADLTS) [5] whose resolution for the adjacent levels has been progressed compared with the conventional deep level transient spectroscopy (DLTS) [6].

2. Principle of SADLTS measurement

SADLTS has been employed to analyse deep levels in the HgCdTe devices. SADLTS is one of the modified DLTS methods analysing the transient capacitance waveform induced by the change in the depletion layer. The transient capacitance waveform is defined as the following expression to solve the reverse problem which obtains the emission rate spectrum $S(\lambda)$ from the transient waveform [5]

$$C(t) = \int_a^b S(\lambda)\exp(-\lambda t)d\lambda, \qquad (1)$$

where λ stands for the emission rate. a and b denote the lower and upper limits in the analysed region of emission rate, respectively. Here λ is expressed as follows

$$\lambda = \sigma v_{th} N_c g \exp(-E_t/kT). \qquad (2)$$

Equation (1) has the form of Volterra integral equation of the first kind. This reverse problem can be solved using the program "CONTIN" written in FORTRAN IV [7-9]. Even if the ratio of amplitudes is more than 100, SADLTS can separate two adjacent components with a ratio of emission rates $\lambda_1/\lambda_2 > 2$ as shown in our previous report [5]. Here λ_1 and λ_2 are emission rates of two adjacent levels, respectively.

3. Sample preparation

Three samples, No. 1, No. 2 and No. 3, were used in this study. These samples were fabricated using molecular beam epitaxy (MBE). The CdTe layer (~ 5 μm thickness) was grown on the (112)B 5° off Si substrate as the buffer layer. (113)B $Hg_{1-x}Cd_xTe$ (~ 13 μm thickness) was grown on the buffer layer as the base layer. In was doped into the base layer to form the n–type region. Then (113)B $Hg_{1-x}Cd_xTe$ (~ 3 μm thickness) was deposited onto the base layer as the cap layer. Ag was doped into the cap layer to form the p–type region. The full width at half maximum (FWHM) of X-ray diffraction, composition of Cd, p– and n–layer thickness, carrier concentrations are listed in Table 1. From the value of FWHM in Table 1, it is seen that this $Hg_{1-x}Cd_xTe$ has the superior crystallinity.

Table 1. Values of the $Hg_{1-x}Cd_xTe$ using the mesa-type diode fabrication.

	Value
FWHM (s)	96
Composition x	0.222
p–HgCdTe thickneess (μm)	3.2
n–HgCdTe thickneess (μm)	13.7
p–carrier concentration (cm^{-3})	1.60×10^{17}
n–carrier concentration (cm^{-3})	6.30×10^{15}

Then the mesa structure was formed by ion milling until the p–n junction was separated. The sample was then etched by Br-methanol to remove the damaged layer induced by ion milling and ZnS was deposited as a protective layer over the entire cap layer using the electron-beam in MBE equipment. Au/Ti was used as both p– and n–side electrodes. Each value of used samples is shown in Table 2, and the diode structure is shown in Fig. 1. From Table 2, it is seen that No. 1 has the largest value of R_0A and No. 3 has the smallest value of R_0A.

Table 2. Specification of mesa-type diodes.

	No. 1	No. 2	No. 3
Chip size (mm^2)	3.5	3.5	3.5
Mesa height (μm)	8	8	8
Diode size (μm^2)	150	150	50
R_0 (Ω)	9.62×10^5	5.28×10^5	4.09×10^6
R_0A (Ω cm^2)	216	118	102
Cutt-off wave length (μm)	10.5	10.5	10.5

4. Measurement

4.1. Current-voltage and differential resistance-voltage characteristics

Diodes characteristics were measured at 78.5 K which was the operating temperature region for the photoconduction detectors using HgCdTe. The applied voltage ranged from –0.2 V to +0.2 V.

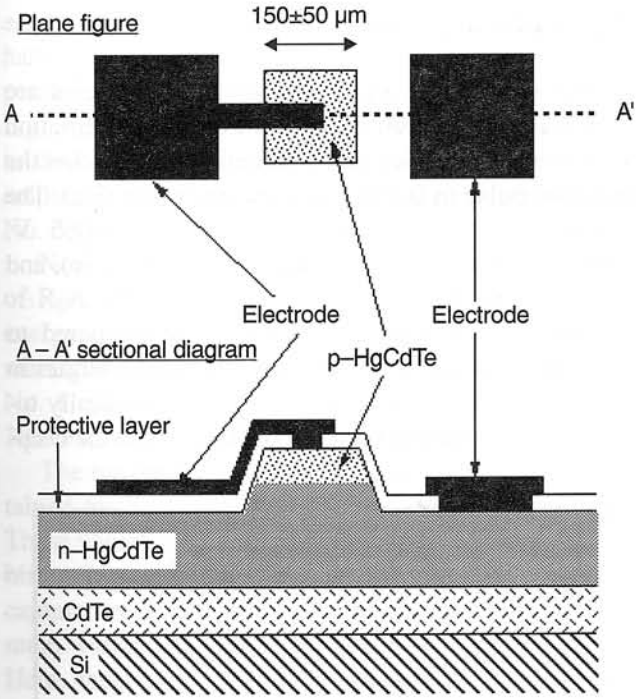

Fig. 1. Scheme of mesa-type HgCdTe device. ZnS and Au/Ti were used as the protective layer and electrodes for both p– and n–side, respectively. A mesa structure was formed by ion milling.

4.2. SADLTS measurement

Samples were mounted in a cryostat and cooled down to the starting temperature. DLTS TEST SYSTEM (SANWA: MI-401) was used to apply the injection bias pulse and to measure the capacitance of samples. The injection pulse was applied to a sample, and then the data of transient capacitance waveforms were logarithmically sampled and stored into a memory. The temperature was changed by a He compressor using a computer and temperature controller. The final digital data of transient capacitance waveforms and temperature were sent to the computer and analysed by the program "CONTIN" to estimate the emission rate spectrum S(λ). The SADLTS measurements were carried out in the temperature region from 26 K to 80 K varied in 2 K steps under the following conditions; amplitudes of bias voltage: 0.005 V (measurement Nos. 1, 5, and 9), 0.065 V (measurement Nos. 2, 6, and 10), 0.080 V (measurement Nos. 3, 7, and 11) and 0.090 V (measurement Nos. 4, 8, and 12), injection pulse bias: –0.1 V, injection pulse width: 1 ms. Here, the measurement numbers from 1 to 4, from 5 to 8 and from 9 to 12 denote the measurements of the sample No. 1, No. 2, and No. 3, respectively.

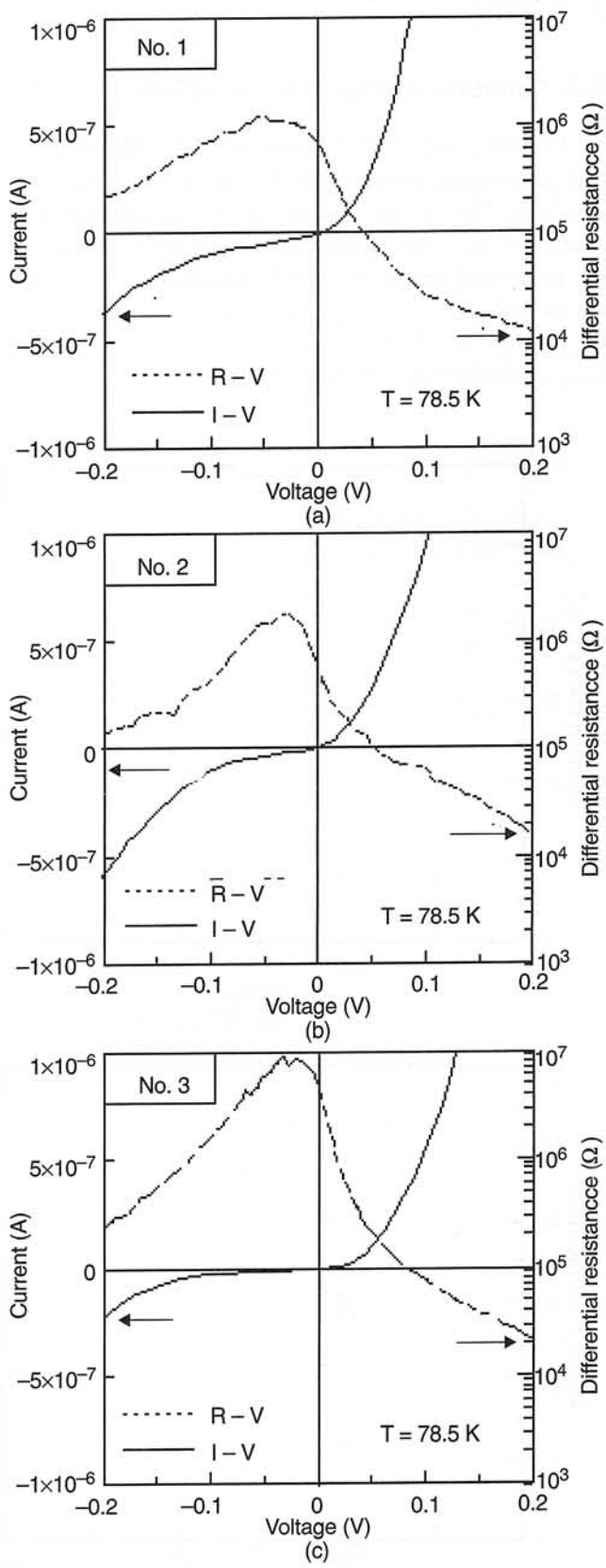

Fig. 2. Current-voltage (I–V) and differential-resistance voltage (R–V) characteristics for samples (a) No. 1, (b) No. 2 and (c) No. 3, respectively.

5. Results

5.1. Current-voltage characteristics

The obtained current-voltage (I–V) and differential resistance-voltage (R–V) characteristics are shown in Fig. 2. All samples show the superior I–V characteristics. The dark currents of each sample in the measured region for the SADLTS measurements are as follows
$I_{No.1} = -9\times10^{-8}$ A, $I_{No.\,2} = -1\times10^{-7}$ A, and
$I_{No.3} = -3\times10^{-8}$ A, respectively.

5.2. SADLTS measurement

The estimated values of activation energies are shown as the function of R_0A in Fig. 3. The variation of activation energies as the function of R_0A for the injection pulse of 0.050 V are shown in Fig. 3(a). The relationships for the injection pulse of 0.065 V, 0.080 V, and 0.090 V are shown in Fig. 3(b), (c), and (d), respectively.

Here, the activation energies were compared to each other, noting the maxima and minima energies in Fig. 3. The shallowest levels shift monotonically toward deeper with the increase of R_0A, while the deep-

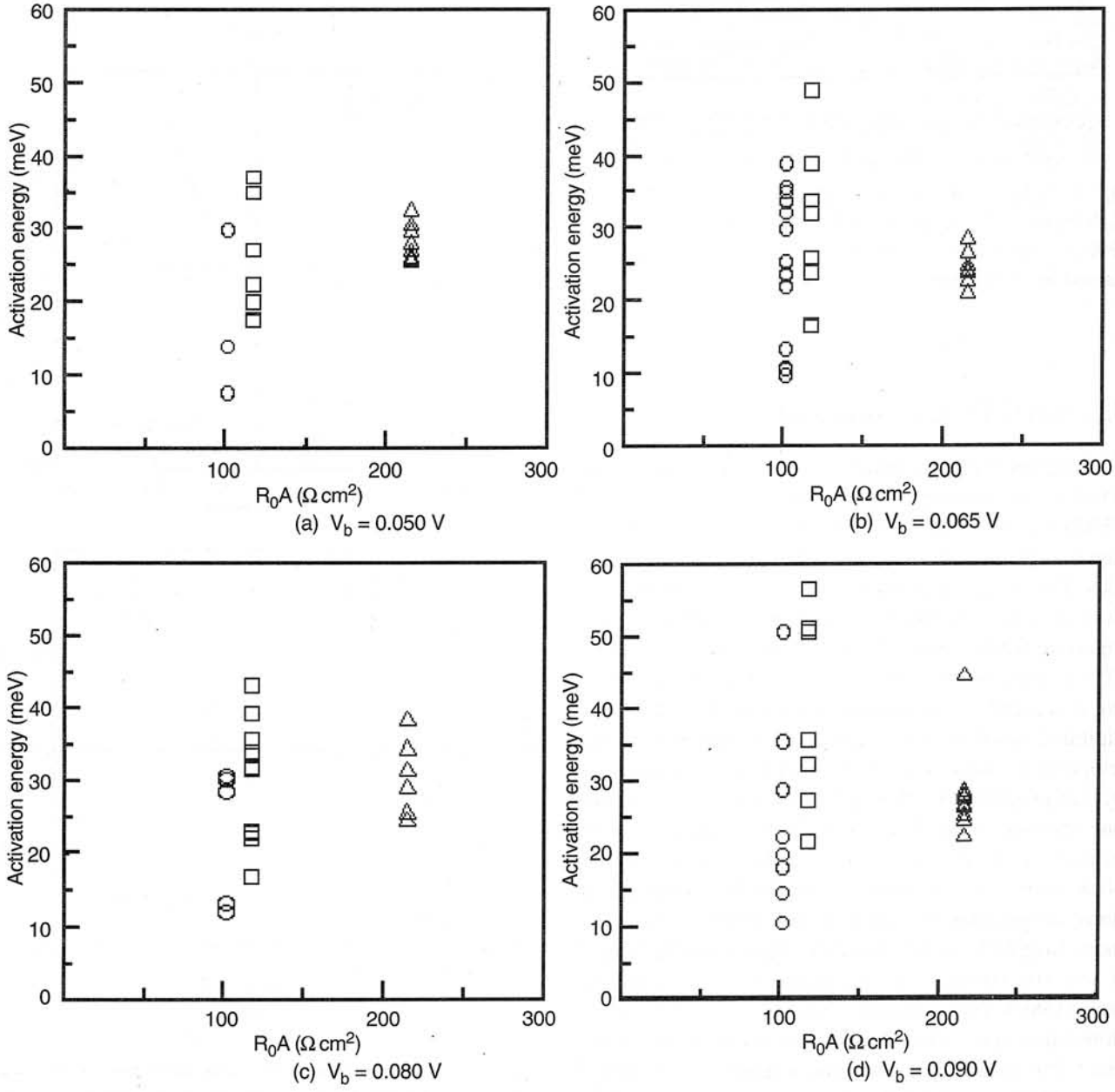

Fig. 3. The relationships between evaluated activation energies and R_0A for the various injection pulse amplitudes. The symbols Δ, □ and o denote the results for No. 1, No. 2 and No. 3, respectively.

est levels have the extrema at 118 $\Omega\,cm^2$. On the other hand, it is seen that there is little injection pulse dependence of the shallowest activation energies in Fig. 3. However, the deepest activation energies shift to deeper level with the increase of injection pulse amplitude, in particular in the case of the sample No. 3.

Noting distributions of deep levels as the function of R_0A, the broadening of distribution of activation energy decrease with the increase of R_0A. The remarkable feature is that deep levels in the sample No. 1, which has the largest R_0A, are obtained near 30 meV for all injection pulse conditions (Fig. 3).

The ranges for values of capture cross sections obtained by SADLTS analysis are shown in Table 3. These values are bundled with respect to all measured bias pulse amplitudes for each sample. The ranges of capture cross sections are quite wide and the maximum values for each sample are extremely large. Here, these extremely huge values of capture cross sections were yielded in the measurement whose amplitude of applied bias voltage was 0.090 V. On the contrary, the minimum values of them were yielded in all measurement conditions.

Table 3. Capture cross sections obtained by SADLTS analysis.

Capture cross sections (cm^2)	
No. 1	10^{-19}~10^{-11}
No. 2	10^{-21}~10^{-9}
No. 3	10^{-20}~10^{-11}

6. Discussion

Various deep levels of HgCdTe have been reported in literatures [10–13], including midgap levels in the band gap. However, the distributions of activation energies of deep levels have not been referred apparently. On the other hand, deep levels have been distributed around E_c–30 meV ranging from E_c–7 meV to E_c–56 meV due to SADLTS having the high resolution for the emission rates in this study. Here, E_c denotes the conduction band edge.

Deep levels in the n–type HgCdTe whose Cd composition x is similar to our samples, x ~ 0.22, have been investigated using magneto-optical spectroscopy (MOS) by Litter *et al.* [12] According to them, the obtained levels were 10 meV and 26 meV corresponding to a quarter of the band gap ($1/4E_g$).

In this study, levels obtained commonly for all injection pulse conditions were E_c–2 meV, E_c–27 meV and E_c–28 meV for No. 1, E_c–22 meV and E_c–32 meV for No. 2, and E_c–30 meV for No. 3, respectively. These levels are considered as $1/4E_g$ by the following equation [14]

$$E_g = -0.302+1.93x-0.81x^2+0.832x^3 +(5.32\times10^{-4})(1-2x)[(-1822+T^3)/(255.2+T^2)]. \quad (3)$$

Here, this region corresponding to $1/4E_g$ is called "region I". On the other hand, the region between E_c–30 meV and the midgap is called "region II" and the region shallower than E_c–30 meV is called "region III". These regions in the band gap are illustrated in Fig. 4.

Deep levels located in the region I have been confirmed in literatures. Therefore, these levels in this region are inherent levels in HgCdTe. This origin is considered to be Te vacancies during the growth process of the HgCdTe crystal.

The region II corresponds to the midgap level. These levels are attributed to the lattice mismatch between HgCdTe and the Si substrate. Levels near the midgap are related to the trap-assisted tunnelling current.

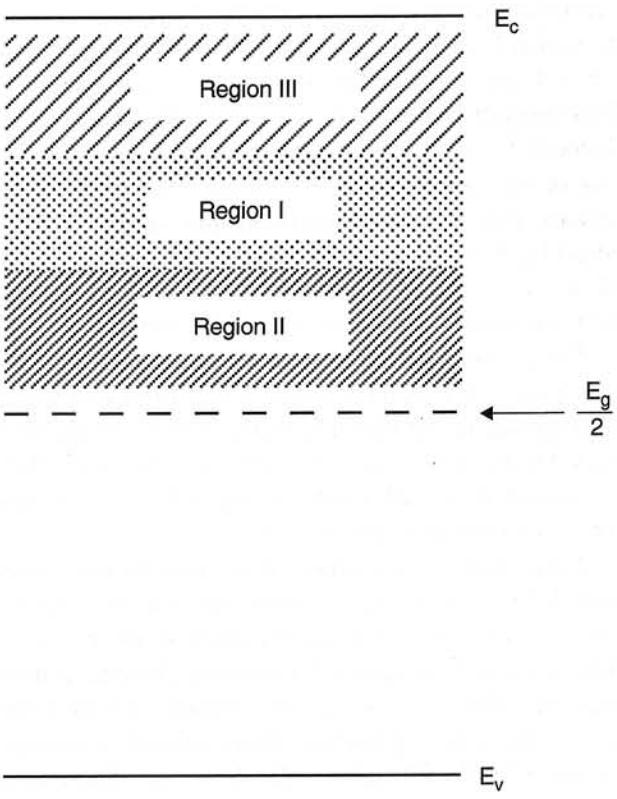

Fig. 4. Scheme of regions existing in the band gap. Deep levels existing in the region I locate round 30 meV. Region II and III range 30 meV ~ midgap and 7 meV ~ 30 meV, respectively.

The region III ranges from E_c–7 meV to E_c–17 meV. These levels have not been confirmed in the planar type HgCdTe investigated by Litter *et al.* [12]. Thus, the region III may be inherent level in the mesa type HgCdTe. The mesa type HgCdTe devices were subjected to the damage due to chemical etching and to ion milling in the fabrication process. This is one of the reasons for the introduction of levels in the region III. Furthermore, doped impurities to control the conduction type of devices may be another origin of levels in the region III. In the measured temperature region, the corresponding thermal energy is about 10 meV, so doped impurities may act as the deep level centres.

Next, let us consider the relationships between R_0A and deep levels. The performance of photodiode is high when its R_0A is large because there is less dark current in the diode. Hence, it suggests that there are some relationships between them. As shown in Fig. 3, activation energies are concentrated around E_c–30 meV when R_0A become large. This is independent of the variation of injection pulse amplitudes.

Many deep levels exist in the region I, but a few deep levels exist in the region II for the sample No. 1. Moreover, there are no levels in the region III. According to these evidences, it can be seen that the dark current in the sample No. 1 is influenced by deep levels in the region I. Deep levels in the sample No. 2 exist in the region I and II, while few levels exist in the region III. This suggests that the dark current in this sample is influenced by deep levels in the regions I and II. In the case of the sample No. 3, deep levels exist in the whole regions, thus the dark current in this sample is influenced by deep levels in the regions I, II, and III. After all, it can be referred that the influence of deep levels in the region I becomes dominant with the increase of R_0A.

Deep levels in the region I are considered to be native levels for HgCdTe, so the effect from this region may remain in the HgCdTe diode in spite of the large R_0A. On the other hand, the influences from levels in the region II and III should be considered to become weak with the increase of R_0A.

Large values of capture cross sections may mean that the values of capture cross section are widened owing to the effect of leakage current in the p–n junction, such as trap assisted tunnelling current, generation-recombination current and surface current. Especially, the value of capture cross section is strongly subjected to the effect from the deviation of activation energy because activation energy is the factor of exponential in Eq. (2) providing the capture cross section. Therefore, this may be attributed to the widened values of capture cross section.

7. Conclusions

The relationships between deep levels related to the dark current in HgCdTe and R_0A which represents the junction performance of photodiodes has been investigated by SADLTS and I–V measurement. The results showed that the distribution of activation energies were centred around E_c–30 meV and ranged from E_c–7 meV to E_c–56 meV in the band gap. Some common activation energies for different injection pulse amplitudes condition were obtained in each sample.

The levels around E_c–30 meV in the region I are considered to be native levels in HgCdTe because they have been confirmed in the planar-type ones. Deep levels in the region II are related to the trap-assisted tunnelling current and attributed to the lattice mismatch between HgCdTe and the Si substrate. Deep levels in the region III have not been confirmed in the planar-type HgCdTe. Thus, these deep levels are specific levels for the mesa-type HgCdTe and may be attributed to the damage induced by ion milling or chemical etching. Furthermore, doped impurities in the HgCdTe may be one of the origins for these levels.

The relationships between deep levels and R_0A have been also studied. The results show that deep levels in the region I are dominant when R_0A become large. This evidence suggests that deep levels in region I are native for the HgCdTe diodes and exist in the region in spite of the increase of junction characteristics.

References

1. J. Yoshino, J. Morimoto, and H. Wada, "Study of deep levels in mesa-type HgCdTe device", *Jpn. J. Appl. Phys.* **37**, 4027–4031 (1998).
2. A. Rogalski, "Photovoltaic detectors", in *Infrared Photon Detectors*, p. 51, edited by A. Rogalski, SPIE Optical Engineering Press, Bellingham, 1995.
3. Ajisawa and N. Oda, "Improvement in HgCdTe diode characteristics by low temperature post-implantation annealing", *J. Electron. Mater.* **24**, 1105–1111 (1995).
4. A. Rogalski, "Photovoltaic detectors", in *Infrared Photon Detectors*, p. 51, edited by A. Rogalski, SPIE Engineering Press, Ballingham, 1995.
5. J. Morimoto, M. Fudamoto, K. Tahira, T Kida, S. Kato, and T. Miyakawa, "Spectral analysis of deep level transient spectroscopy (SADLTS)", *Jpn. J. Appl. Phys.* **26**, 1634–1640 (1987).

6. D.V. Lang, "Deep level transient spectroscopy: a new method to characterise traps in semiconductors", *J. Appl. Phys.* **45**, 3023–3032 (1974).
7. S.W. Provencher,"A constrained regularisation method for inverting data represented by linear algebraic or integral equations", *Comput. Phys. Commun.* **27**, 213–227 (1982).
8. S.W. Provencher, "Contin: a general purpose constrained regularisation program for inverting noisy linear algebraic and integral equations", *Comput. Phys. Commun.* **27**, 229–242 (1982).
9. S.W. Provencher, *Contin Users Manual*, European Molecular Biology Laboratory, Heidelberg, 1982.
10. D.L. Polla and C.E. Jones, "Deep level transient spectroscopy in $Hg_{1-x}Cd_xTe$", *Solid State Commun.* **36**, 809–812 (1980).
11. D.L. Polla and C.E. Jones, "Deep level studies in $Hg_{1-x}Cd_xTe$. I: Narrow-band-gap space-charge spectroscopy", *J. Appl. Phys.* **5**, 5118–5131 (1981).
12. C.L. Litter, D.G. Seiler, and M.R. Loloee,"Magneto-optical investigation of impurity and defect levels in HgCdTe alloys", *J. Vac. Sci. Technol.* **A8**, 1133–1138 (1991).
13. M.C. Chen and R.A. Schebel, "Observation of a deep level in p-type $Hg_{0.78}Cd_{0.22}Te$ with high dislocation density", *J. Appl. Phys.* **71**, 5269–5271 (1992).
14. J.R. Lowney, D.G. Seiler, C.L. Litter, and I.T. Yoon, "Intrinsic carrier concentration of narrow-gap mercury cadmium telluride based on the non-linear temperature dependence of the band gap", *J. Appl. Phys.* **71**, 1253–1258 (1992).